Title

Umbilical cord blood metabolomics reveal distinct signatures of dyslipidemia prior to bronchopulmonary dysplasia and pulmonary hypertension

Journal

American Journal of Physiology - Lung Cellular and Molecular Physiology, 315(5)

ISSN

1040-0605

Authors

La Frano, Michael R

Fahrmann, Johannes F

Grapov, Dmitry

et al.

Publication Date

2018-11-01

DOI

10.1152/ajplung.00283.2017

Metabolomics (2017) 13:32
DOI 10.1007/s11306-017-1170-6

ORIGINAL ARTICLE

Metabolic perturbations of postnatal growth restriction and hyperoxia-induced pulmonary hypertension in a bronchopulmonary dysplasia model

Michael R. La Frano[1,2,3] · Johannes F. Fahrmann[1] · Dmitry Grapov[4] · Oliver Fiehn[1,5] · Theresa L. Pedersen[6] · John W. Newman[1,2,6] · Mark A. Underwood[7] · Robin H. Steinhorn[8] · Stephen Wedgwood[7]

Received: 30 September 2016 / Accepted: 30 January 2017

Abstract

Introduction Neonatal pulmonary hypertension (PH) is a common manifestation of bronchopulmonary dysplasia (BPD) and contributes to increased morbidity and mortality of preterm birth. Postnatal growth restriction (PNGR) and hyperoxia are independent contributors to PH development, as indicated by our previous work in a rat model of BPD.

Objective To explore the metabolic consequences of induction of PH with hyperoxia and PNGR in a rat model of BPD.

Methods Sprague–Dawley rat pups (n = 4/group) underwent three modes of PH induction: (1) growth restriction-induced by larger litter size; (2) hyperoxia-induced by 75% oxygen exposure; (3) combined growth restriction and hyperoxia. Primary metabolism, complex lipids, biogenic amines, and lipid mediators were characterized in plasma and lung tissue using GC- and LC-MS technologies.

Results Specific to hyperoxic induction, pulmonary metabolomics suggested increased reactive oxygen species (ROS) generation as indicated by: (1) increased indicators of β-oxidation and mitochondrial respiration; (2) changes in ROS-sensitive pathway activity and metabolites including the polyol pathway and xanthine oxidase pathways, and reduced glutathione; (3) decreased plasmalogens. Unlike the lung, circulating metabolite changes were induction mode-specific or additive in the combined modes (e.g. 1) growth-restriction reduced phosphatidylcholine; (2) hyperoxia increased oxylipins and trimethylamine-N-oxide (TMAO); (3) additive effects on 3-hydroxybutyric acid and arginine.

Conclusion The present study highlights the variety of metabolic changes that occur due to PNGR- and hyperoxia-induced PH, identifying numerous metabolites and pathways influenced by treatment-specific or combined effects. The rat model used in this study presents a robust means of uncovering the mechanisms that contribute to the pathology of PH.

Michael R. La Frano and Johannes F. Fahrmann contributed equally to this work.

Electronic supplementary material The online version of this article (doi:10.1007/s11306-017-1170-6) contains supplementary material, which is available to authorized users.

✉ Stephen Wedgwood
swedgwood@ucdavis.edu

[1] NIH West Coast Metabolomics Center, Davis, CA, USA

[2] Department of Nutrition, University of California Davis, Davis, CA, USA

[3] Department of Food Science and Nutrition, California Polytechnic State University, San Luis Obispo, CA, USA

[4] CDS Creative Data Solutions, Ballwin, MO, USA

[5] Department of Biochemistry, Faculty of Sciences, King Abdulaziz University, Jeddah 21589, Saudi Arabia

[6] USDA-ARS Western Human Nutrition Research Center, Davis, CA, USA

[7] Department of Pediatrics, University of California Davis Medical Center, Research II Building, 4625 2nd Avenue, Sacramento, CA 95817, USA

[8] Department of Pediatrics, Children's National Medical Center, George Washington University, Washington, DC, USA

Published online: 13 February 2017

Keywords Metabolomics · Lipid mediators · Pulmonary hypertension · Bronchopulmonary dysplasia · Hyperoxia · Growth restriction

1 Introduction

Bronchopulmonary dysplasia (BPD) is a chronic lung disease of prematurity that occurs most frequently in preterm infants born before 28 weeks of gestation (Mirza et al. 2014). Pulmonary hypertension (PH) is a common complication of BPD that greatly increases morbidity and mortality of preterm birth (Slaughter et al. 2011; Mourani et al. 2015). PH is often not diagnosed in preterm infants until symptoms emerge after many weeks of life, when the disease is advanced and associated with severe right ventricular cardiac dysfunction (Berkelhamer et al. 2013). While several risk factors for PH have been identified, including growth restriction and extremely low gestational age (Robbins et al. 2012), no reliable biomarkers currently exist. A better understanding of the mechanisms that trigger PH in preterm infants is needed to improve the detection, prevention and treatment of BPD-related PH.

Recent studies have suggested that the origins of PH may begin in fetal life. Rozance et al. studied a placental insufficiency sheep model of fetal growth restriction (FGR) and found significant pulmonary artery endothelial changes, including downregulation of the nitric oxide synthase pathway, which could promote vascular dysfunction and remodeling after birth (Rozance et al. 2011). Moreover, we have recently provided evidence that fetal or postnatal growth restriction contributes independently and interactively in the development of PH (Check et al. 2013; Wedgwood et al. 2016).

Rats serve as valuable models for the study of lung development associated with BPD and FGR because they are born with immature lungs during the saccular and early alveolar stages. A rat model of post-natal growth restriction (PNGR) displays poor growth (body weight 22% lower at 10 days of life and 24% lower at 20 days), altered body composition (25% decrease in body fat at 22 days of life), marked decreases in IGF-1 and leptin, increased glucose tolerance, and poor neurodevelopment (Jou et al. 2013). Using this model, we previously showed that newborn rats under either PNGR or hyperoxia alone or in combination have increased right ventricular hypertrophy (RVH) and medial wall thickness (MWT) in a cumulative fashion, suggesting that both contribute independently to the development of PH (Wedgwood et al. 2016). While the mechanisms by which hyperoxia induces PH are better characterized, the mechanisms driving the cardiopulmonary effects of PNGR remain largely unknown.

The pathophysiology of BPD and PH is known to have a strong metabolic component (Pearson et al. 2001). Therefore, evaluation of metabolic perturbations associated with these developmental lung disorders represents a valuable approach to exploring the contributing factors that influence the underlying pathophysiology of BPD and PH. In the current study, metabolic changes were investigated using a multi-platform metabolomics approach consisting of gas chromatography time-of-flight mass spectrometry (GCTOFMS), ultrahigh performance liquid chromatography quadrupole accurate mass time-of-flight mass spectrometry (UPLC-qTOFMS) and UPLC tandem mass spectrometry (MS/MS). We characterized the metabolome response of plasma and lung tissue using PNGR, hyperoxia, or a combination of these two treatments. We hypothesize that the two modes of PH elicit distinct independent metabolic features that are exacerbated in the combined growth restriction and hyperoxia group. Such knowledge of metabolism is instrumental in further understanding the pathophysiology of BPD and PH and to identify potential mechanisms to be explored in the future.

2 Materials and methods

2.1 Animal cohorts and experimental conditions

Pregnant Sprague Dawley (SD) rats (gestational day 15) were housed in plastic cages under constant conditions. After a 7 day acclimation period, litters were delivered and pups randomly distributed between litters of 10 pups (N, normal intake) or litters of 17 pups (R, restricted intake). Normal and restricted intake pups were exposed to 75% oxygen (O, oxygen) in a Plexiglass chamber or to 21% oxygen (A, room air) continuously for 14 days, with daily rotation of dams to avoid oxygen toxicity. Pups were euthanized by exposure to CO_2 followed by cardiac puncture and exsanguination, and plasma was collected and stored at −80 °C. Lungs were excised, snap-frozen in liquid nitrogen and stored at −80 °C as previously described (Wedgwood et al. 2016). Tissue from random lobes and areas were used for subsequent analysis.

The following four groups were included in the study: room air, normal intake (AN), room air, restricted intake (AR), high oxygen, normal intake (ON), and high oxygen, restricted intake (OR). The study design and methods overview is depicted in Fig. 1a.

2.2 Metabolomic, lipidomic, nitric oxide pathway, and oxylipin analysis

The MiniX database (Scholz and Fiehn 2007) was used as a Laboratory Information Management System (LIMS).

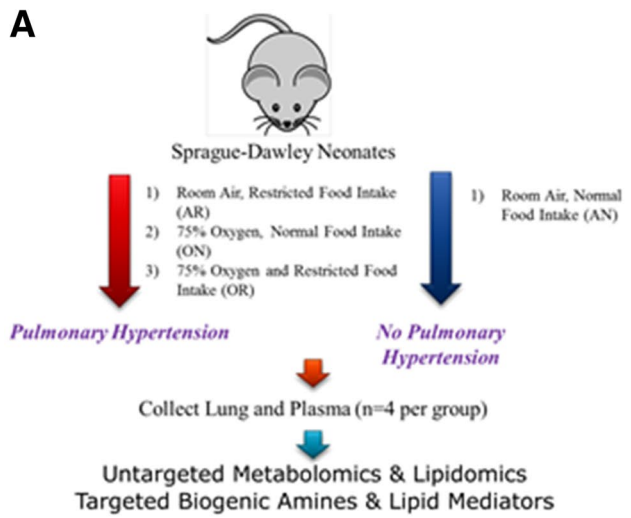

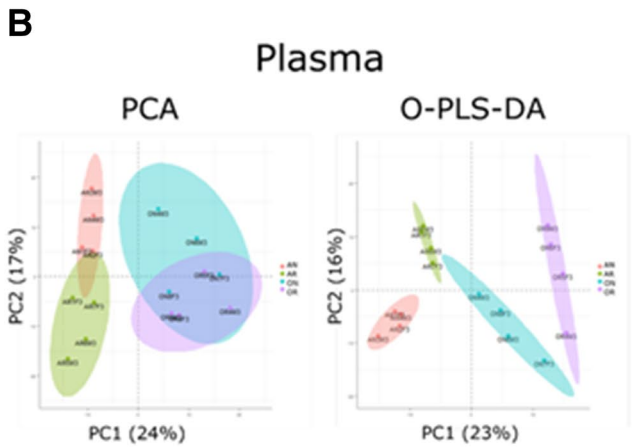

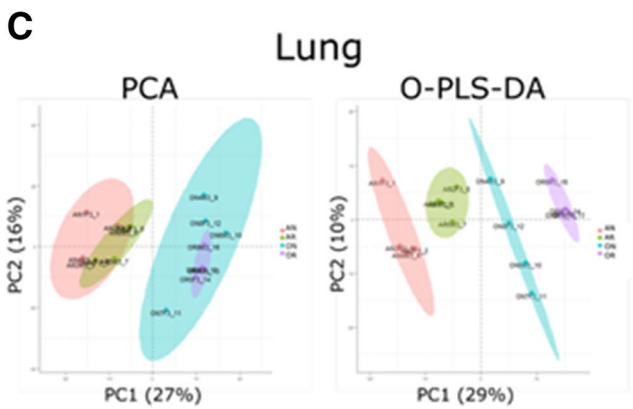

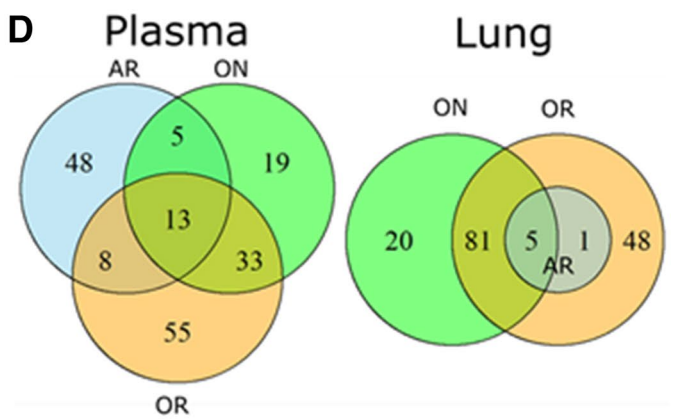

E

PLASMA

Metabolites	PNGR (AR)	Hyperoxia (ON)	Hyperoxia + PNGR (OR)
Combined effects			
Acylcarnitines	-	-	↑
Additive Effects			
Ketone bodies	↑	↑	↑↑↑
Glucogenic/Ketogenic Amino Acids	-	↓↓	↓↓↓
Arginine (NO pathway)	-	↓	↓↓↓
Effects unique to hyperoxia			
Xanthine oxidase metabolites	-	↓	↓↓
Unchanged			
TCA Cycle intermediates	-	-	-
Glycolysis intermediates	-	-	-
Pentose phosphate metabolite	-	-	-
Polyol pathway metabolites	-	-	-
Glutathione (Antioxidant)	-	-	-

LUNG

Metabolites	PNGR (AR)	Hyperoxia (ON)	Hyperoxia + PNGR (OR)
Combined effects			
Ketone bodies	-	-	↑↑↑
Glucogenic/Ketogenic Amino Acids	-	-	↓↓
Effects unique to hyperoxia			
TCA Cycle intermediates	-	↑	↑↑
Glycolysis intermediates	-	↓	↓↓
Pentose phosphate metabolite	-	↓	↓↓
Xanthine oxidase metabolites	-	↓	↓↓
Polyol pathway metabolites	-	↑↑	↑↑
Acylcarnitines	-	↑↑	↑↑
Glutathione (Antioxidant)	-	↓	↓
Unchanged			
Arginine (NO pathway)	-	-	-

Fig. 1 Study Overview. **a** Study design and methods overview; Multivariate analysis of lung and plasma metabolomics data. **a** Principal component analysis (PCA) and orthogonal partial least squares discriminant analysis (O-PLS-DA) are shown for (**b**) plasma and **c** lung metabolomics data for all four experimental conditions. For PCA, the scores for the first two principal components are shown. For O-PLS-DA, two latent variables (LV) with no orthogonal LV (plasma) or one LV (lung) was selected to discriminate between the four groups. O-PLS-DA LV and orthogonal LV was selected using leave-one-out cross validation (Supplemental Table S1); **d** Venn diagrams illustrating the number of significantly different metabolites (raw p-value < 0.05; known only) between AR, ON and OR relative to AN for plasma and lung tissue; **e** Summary of primary metabolite and biogenic amine concentration changes in lung and plasma. Key: ↑ or ↓ different than AN ; ↑↑ or ↓↓ different than AN and AR; ↑↑↑ or ↓↓↓ different than AR and ON (raw $p < 0.05$)

Detailed information on sample preparation and data acquisition for all analytical platforms are reported in Supplementary Material and described briefly below.

For analysis of primary metabolism, plasma aliquots (30 µL) or lung tissue homogenate (5 µg) were extracted, derivatized and metabolite levels were quantified by gas chromatography time-of-flight mass spectrometry (GC-TOFMS) as previously described (Fiehn et al. 2008). Acquired spectra were further processed using the BinBase database (Fiehn et al. 2005; Scholz and Fiehn 2007), filtered (Kind et al. 2007), and matched against the Fiehn Mass Spectral Library of 1200 authentic metabolite spectra.

For analysis of complex lipids, samples were extracted as previously described (Fahrmann et al. 2015). Briefly, they were extracted through sequential addition of 225 µL of chilled methanol, 750 µL of chilled methyl tertiary butyl ether (MTBE, Sigma Aldrich) containing the internal standard 22:1n9 cholesteryl ester and 188 µL of ultrapure water. The upper (non-polar) layer was dried, then resuspended in methanol:toluene (90:10) containing 50 ng/mL 1-cyclohexylureido,3-dodecanoic acid (CUDA; Sigma Aldrich) and analyzed on an 1290 A Infinity UPLC and Accurate Mass 6530-QTOFMS (Agilent Technologies; Santa Clara, CA) in both positive and negative mode. Data were processed using MZmine 2.10 and reported as peak heights for the quantification ion (m/z) at the specific retention time for each annotated and unknown metabolite.

For analysis of biogenic amines, including targeted analysis of arginine, citrulline and ornithine, half of the polar (bottom) layer from the lipid extract was dried and resuspended in 60 µL of 80:20 acetonitrile (ACN)//H2O containing the internal standards CUDA, L-arginine-$^{15}N_2$ (Cambridge Isotope Laboratory, Inc.), and Val-Tyr-Val (Sigma Aldrich). Resuspended samples were analyzed on a 1290 A Infinity UPLC system with a 6530 QTOFMS (Agilent Technologies) in positive ionization mode. Agilent MassHunter Workstation Software was used to quantify peak heights.

Plasma non-esterified oxylipins were isolated using a Waters Ostro Sample Preparation Plate (Milford, MA). Aliquots of 50 µL plasma were extracted. Briefly, plasma aliquots were added to the plate wells and spiked with a 5 µL anti-oxidant solution (0.2 mg/ml solution BHT/EDTA in 1:1 MeOH:water) and 5 µL 1000 nM analytical deuterated surrogates. ACN (150 µL) with 1% formic acid was forcefully added to the sample, eluted with vacuum, dried, then re-constituted with the internal standards CUDA and 1-phenyl 3-hexadecanoic acid urea (PHAU) at 100 nM (50:50 MeOH:ACN), and filtered (0.1 µm) before analysis.

For the targeted analysis of total alkaline stable oxylipins (esterified and non-esterified species) lung tissue was processed as previously reported (Picklo and Newman 2015). Briefly, rat lung samples (~25 mg) were extracted with 10:8:11 cyclohexane:2-propanol:1 M ammonium acetate, incubated with 100 µL 0.5 M sodium methoxide for 1 h at 60 °C to trans-esterify oxylipins, and diluted with 100 µL H2O and incubated 30 min at 60 °C to yield oxylipin free acids which were isolated using 10 mg Oasis HLB solid phase extraction column (Waters Corp, Milford, MA) prior to analysis.

Analytes in 50 µL extract aliquots were separated as described previously (Strassburg et al. 2012; Grapov et al. 2012) on a Waters Acquity UPLC and detected by negative mode electrospray ionization using multiple reaction monitoring on an API 4000 QTrap (AB Sciex, Framingham, MA). Analytes were quantified using internal standard methods and 5–7 point calibration curves ($r2 \geq 0.997$). Calibrants and isotopically labeled surrogates were either synthesized or purchased from Cayman Chemical (Ann Arbor, MI) or Larodan Fine Chemicals (Malmo, Sweden). Data were processed with AB Sciex MultiQuant version 3.0.

2.3 Data analysis

Univariate statistical analyses and other statistical details can be found in Supplementary Material. Briefly, univariate statistical analyses were performed using one-way analysis of variance (ANOVA) on $\log_{10}$ transformed values. The significance levels (i.e. p-values) were adjusted for multiple hypothesis testing according to Benjamini and Hochberg (Benjamini and Hochberg 1995) at a false discovery rate (FDR) of 0.05. Tukey HSD posthoc test was used to determine pairwise group differences. All univariate analysis was performed using DeviumWeb (DeviumWeb 2014).

Multivariate modeling was conducted using principal component analysis (PCA) and orthogonal signal correction partial least squares discriminant analysis (O-PLS-DA) (Svensson et al. 2002) with DeviumWeb. Only metabolites with known annotations were included in the multivariate modeling. Model performance is provided in Supplemental Table S1.

A Venn diagram was used to illustrate the number of unique and similar metabolic differences (Tukey HSD p-value < 0.05) between treatment groups relative to control.

Network analysis was used to investigate statistical results for primary metabolites (GCTOF) and polar metabolites (LCqTOF-HILIC) within a biochemical context using KEGGs, PubChem, and MetaMapR, as detailed in Supplementary information, (Barupal et al. 2012; Kotera et al. 2012; Bolton et al. 2008; Dmitry; Grapov 2014; Cao et al. 2008) and visualized using Cytoscape (Shannon et al. 2003).

Spearman rank correlations were conducted between circulating and lung metabolites in Prism Software v5.0 (GraphPad Software Inc., La Jolla, CA). Box-and-whisker

plots (Supplemental Figure S3) for complex lipids and lipid mediator data were produced in Metaboanalyst 3.0 (Xia and Wishart 2016).

All raw data can be accessed through the NIH Metabolomics Workbench (Sud et al. 2015). All study data and results can be viewed in Supplemental Table S2.

3 Results

3.1 Body weight

Final AR and OR body weights (26.0 ± 0.9 g and 24.1 ± 1.5 g, respectively) were significantly lower ($P < 0.001$) than the AN and ON groups (37.6 ± 2.6 g and 34.0 ± 1.9 g, respectively). Exposure to hyperoxia did not affect body weight in control or PNGR pups. Phenotypic measurements of disease presence including pulmonary arterial pressure, comparative ventricle thickness (Fulton's Index), vessel density, and MWT have been previously published (Wedgwood et al. 2016).

3.2 Analysis of the metabolome

A total of 501 and 509 known metabolites were detected in plasma and lung tissue, respectively (Supplemental Table S2). PCA and O-PLS-DA were used to evaluate and visualize sample class structure using all known metabolites (Fig. 1b, c). A clear separation of the groups is observed with OR being the most different from control (AN) in both lung tissue and plasma. A Venn diagram was used to generalize the number of unique and similar significant metabolic differences between the three experimental conditions compared to control (AN) (Fig. 1d).

3.3 Growth restriction and hyperoxia elicit perturbations in primary metabolites

Evaluation of pulmonary primary metabolites and biogenic amines revealed profound differences in the lung metabolome between either ON or OR relative to control but minimal differences between growth restriction (AR) and control (AN) (Fig. 2). The number of significantly different metabolites ($p < 0.05$) were most pronounced in the combined (OR) group, consistent with the PCA and O-PLS-DA multivariate modeling. Figure 1e summarizes the directional concentration changes in significantly different metabolites from various metabolic pathways in order to note observed combined, additive, and hyperoxia-specific effects of the treatments. Specifically, compared to AN, lung tissue from the OR group exhibited: (1) decreases in glycolytic intermediates glucose-6-phosphate and fructose-6-phosphate (2) increases in tricarboxylic acid (TCA) cycle intermediates succinic acid, malic acid and fumaric acid, (3) decreases in several glucogenic amino acids such as methionine, aspartic acid, and valine, and an elevation in cysteine, (4) reduction in glutathione, (5) increases in several sugar alcohols including sorbitol, xylitol, and 1,5-anhydroglucitol and unchanged glucose, (6) increases in several organic acids led by 3-hydroxybutyric acid, (7) reductions in nucleotides, particularly the purines xanthosine, xanthine and uric acid, (8) reductions in cholesteron-3-ol and cholesterol and (9) elevations in free fatty acids and the short-chain acylcarnitines. Many of these changes were similarly observed in ON compared to control. The trend towards lower arginine concentration in the hyperoxia groups was not significant ($P < 0.13$).

Consistent with the observations in the lung, many of the aforementioned primary metabolites exhibited similar tendencies (increased/decreased) in the plasma (Fig. 3). A commonality which was observed between all three experimental groups relative to control were elevations in select circulating free fatty acids, acylcarnitines and 3-hydroxybutyric acid. Plasma arginine was found to be significantly reduced in the hyperoxic groups. Interestingly, TMAO was elevated in the OR versus all other groups.

3.4 Growth restriction and hyperoxia induce distinct differences in lipid profiles

Evaluation of the lipidome of lung tissue and plasma revealed prominent differences between growth restriction and hyperoxia. In the lung, summed triacylglycerides, cholesterol esters, plasmalogen-phosphatidylcholines (PCs), lysophosphatidylcholines (LPCs) and plasmalogen-phosphatidylethanolamines were found to be uniquely reduced in the ON and OR compared to control (Supplemental Figure S1A), while circulating PCs and LPCs were found to be significantly reduced in AR and OR compared to control (Supplemental Figure S1B). Like the AR group, sphingomyelins (SMs), LPCs, glucosylceramides and plasmalogen-LPCs tended to be lower in OR compared to control.

3.5 Hyperoxia elicits alterations in lipid mediators

Lipid signaling mediators (oxylipins) were almost exclusively altered by hyperoxia treatment in both the lung and plasma. Total (esterified and non-esterified) lung cytochrome p450-derived oxylipins were elevated such as 14(15)-EpETrE and 16(17)-EpDPE, while others appeared to increase including 11(12)-EpETrE, 8(9)-EpETrE, and 20-HETE ($p < 0.1$) (Fig. 4). 6-keto-PGF1α was elevated in all treatment groups. Numerous 12/15-LOX products 12-HEPE, 15-HEPEs, 8(15)-DiHETE, 13-HOTE, and 17-HDoHE were significantly reduced in ON and OR relative to control. The oxylipins 9-HETE

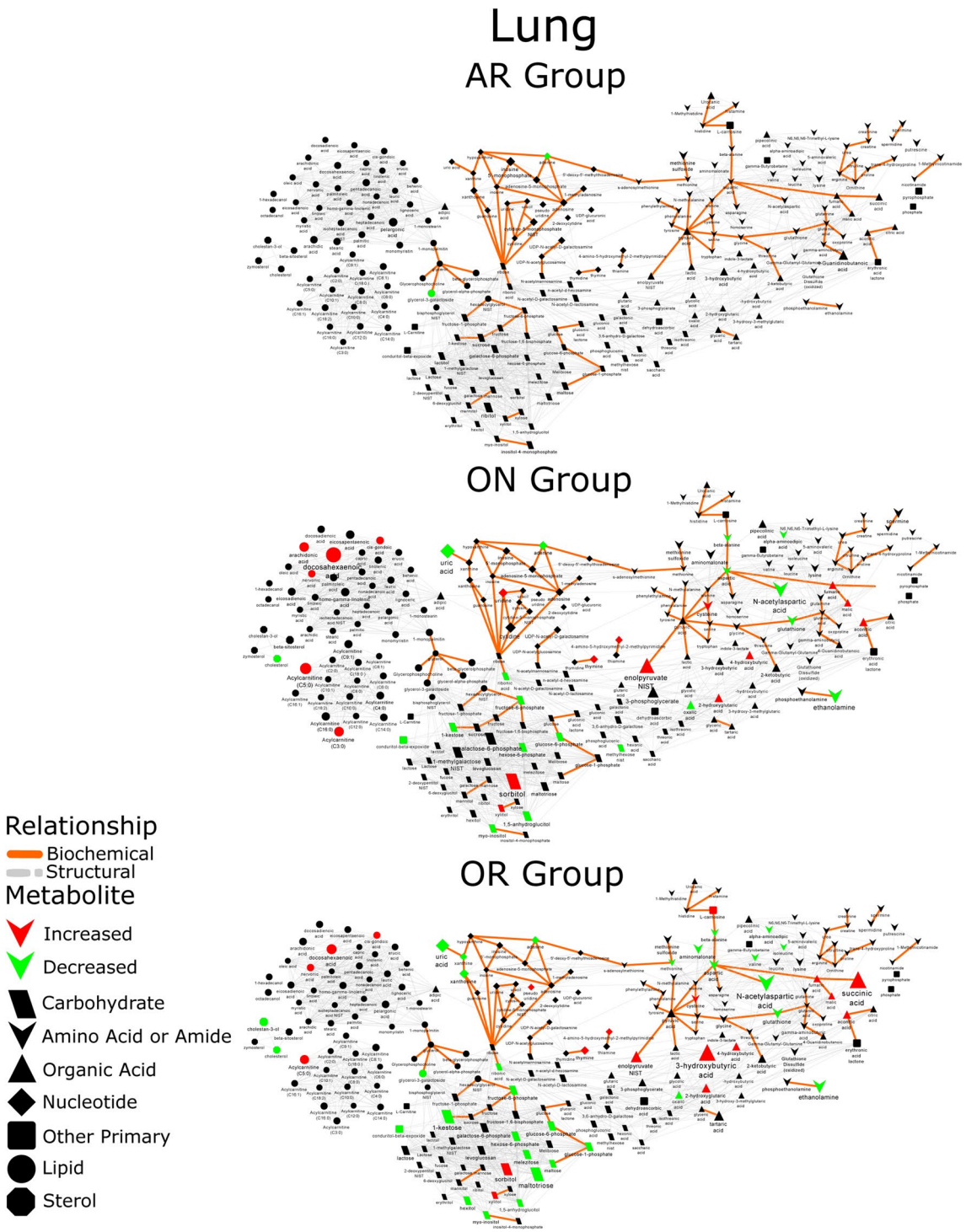

Fig. 2 Biochemical network displaying differences in lung tissue primary metabolites and biogenic amines between AR, ON and OR compared to AN. Edge color and shape depict relationship between nodes [*solid orange*: biochemical KEGG Reactant Pairs; *broken grey*: structural similarity, tanimoto coefficient (≥0.7)]. Node color represents significance (*black*-not statistically different; *green*- significantly decreased in group relative to AN; *red*- significantly increased in group relative to AN). Node and node label size reflect absolute fold change of experimental group relative to AN. Node shape depicts major biochemical domain of respective metabolite. AN- normal food intake, normal air; AR- restricted food intake, normal air; ON- 75% oxygen, normal food intake; OR- 75% oxygen, restricted food intake

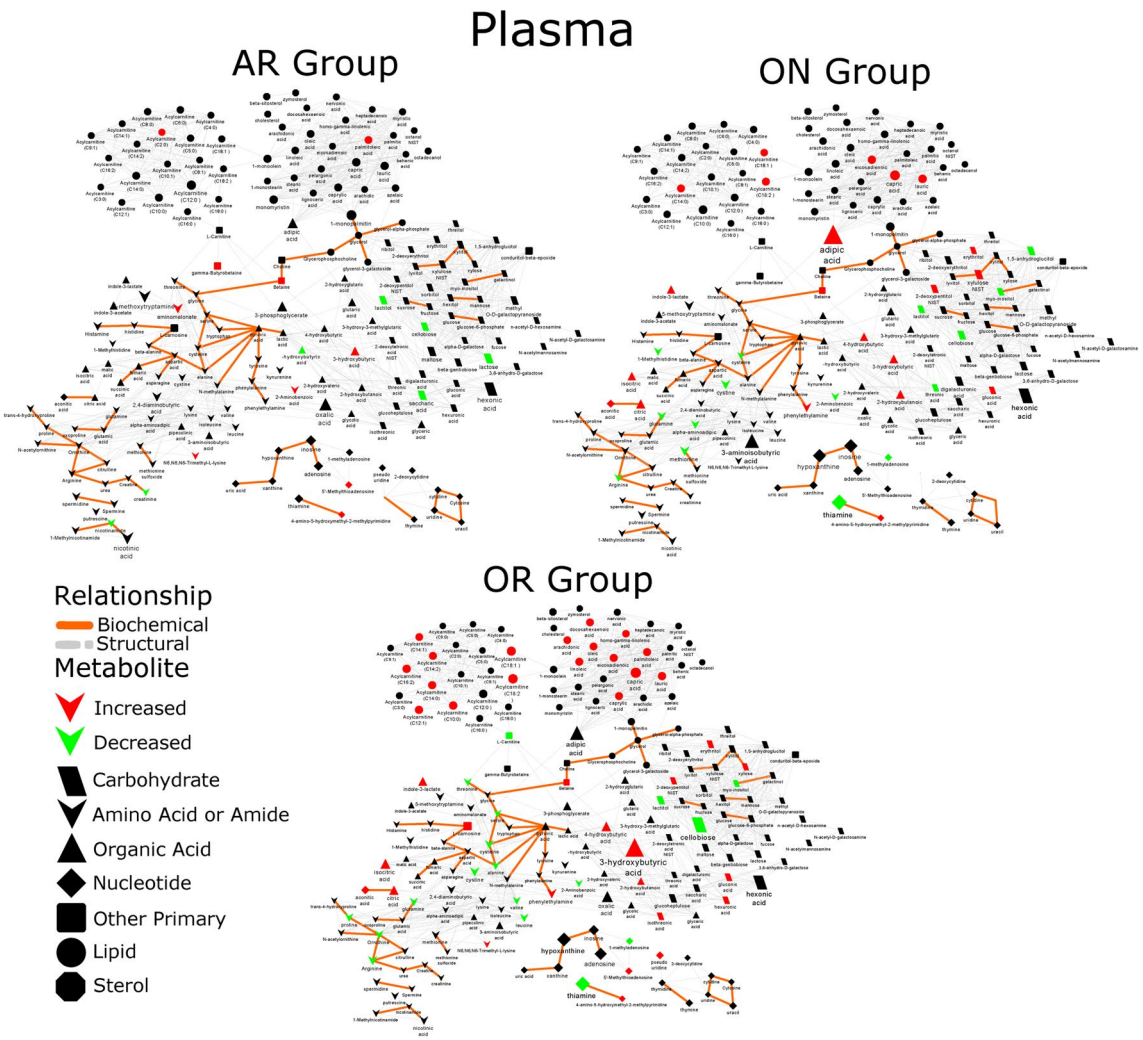

Fig. 3 Biochemical network displaying differences in circulating primary metabolites and biogenic amines between AR, ON and OR compared to AN. Edge color and shape depict relationship between nodes [*solid orange*: biochemical KEGG Reactant Pairs; *broken grey*: structural similarity, tanimoto coefficient (≥0.7)]. Node color represents significance (*black*-not statistically different; *green*- significantly decreased in group relative to AN; *red*- significantly increased in group relative to AN). Node and node label size reflect absolute fold change of experimental group relative to AN. Node shape depicts major biochemical domain of respective metabolite. AN- normal food intake, normal air; AR- restricted food intake, normal air; ON- 75% oxygen, normal food intake; OR- 75% oxygen, restricted food intake

and $PGF2_{\alpha}$ isoprostanes, markers of lipid peroxidation, were not different between groups.

In regards to non-esterified oxylipins in plasma, several circulating soluble epoxide hydrolase (sEH)-derived diols including 5,6-DiHETrE, 8,9-DiHETrE, 11,12-DiHETrE, 14,15-DiHETrE, 17,18-DiHETE and 14,15-DiHETE were differentially elevated in the ON and OR groups while epoxides were largely unchanged or not detected (Fig. 5), collectively suggesting increased sEH activity as supported by elevated 14,15-DiHETrE/14(15)-EpETrE ratio ($P < 0.01$), a proxy of sEH activity (Luria et al. 2007). Similarly, 5-LOX-derived 5-HETE, 5-HEPE and 9-HOTE were significantly elevated in ON and OR compared to control.

Supplemental Figures S3A and S3B summarize the key oxylipin changes observed in the lung and plasma and groups them according to the enzymes from which they are derived.

3.6 Growth restriction and hyperoxia induce additive effects on reactive nitrogen species generation

Western blot analysis of lung 3-nitrotyrosine (3-NT) showed increased expression in the AR and ON groups versus control with an additive effect in the OR group (Supplemental Figure S2).

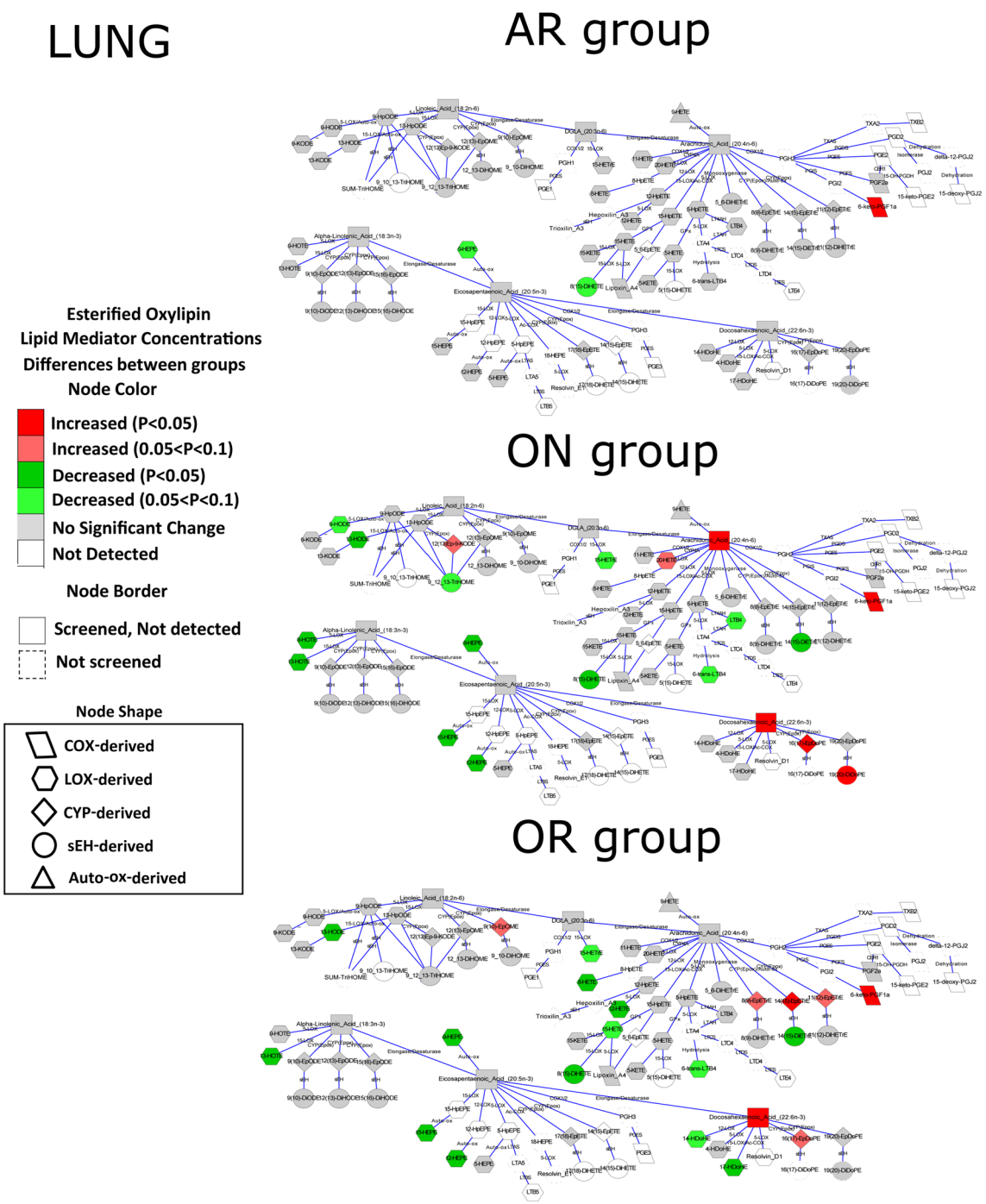

Fig. 4 Biochemical network displaying differences in lung esterified oxylipins between AR, ON and OR relative to AN. Edge label represents the enzymes which mediates the respective biochemical transformation. Node color represents significance (*white*- not detected; *grey*-not statistically different; *green*- significantly decreased in group relative to AN; *red*- significantly increased in group relative to AN). Lighter shades of *red* and *green* were compounds changing with p-values > 0.05 but <0.1. Node shapes depicts the respective oxylipin metabolizing pathway. AN- normal food intake, normal air; AR- restricted food intake, normal air; ON- 75% oxygen, normal food intake; OR- 75% oxygen, restricted food intake

4 Discussion

The current study used metabolomics to further investigate the consequences of BPD and PH in a growth restriction and hyperoxic rat model with demonstrated changes in several PH-related proteins plus RVH, MWT and vessel density (Wedgwood et al. 2016). Specifically, a combined metabolomics approach consisting of untargeted analysis of

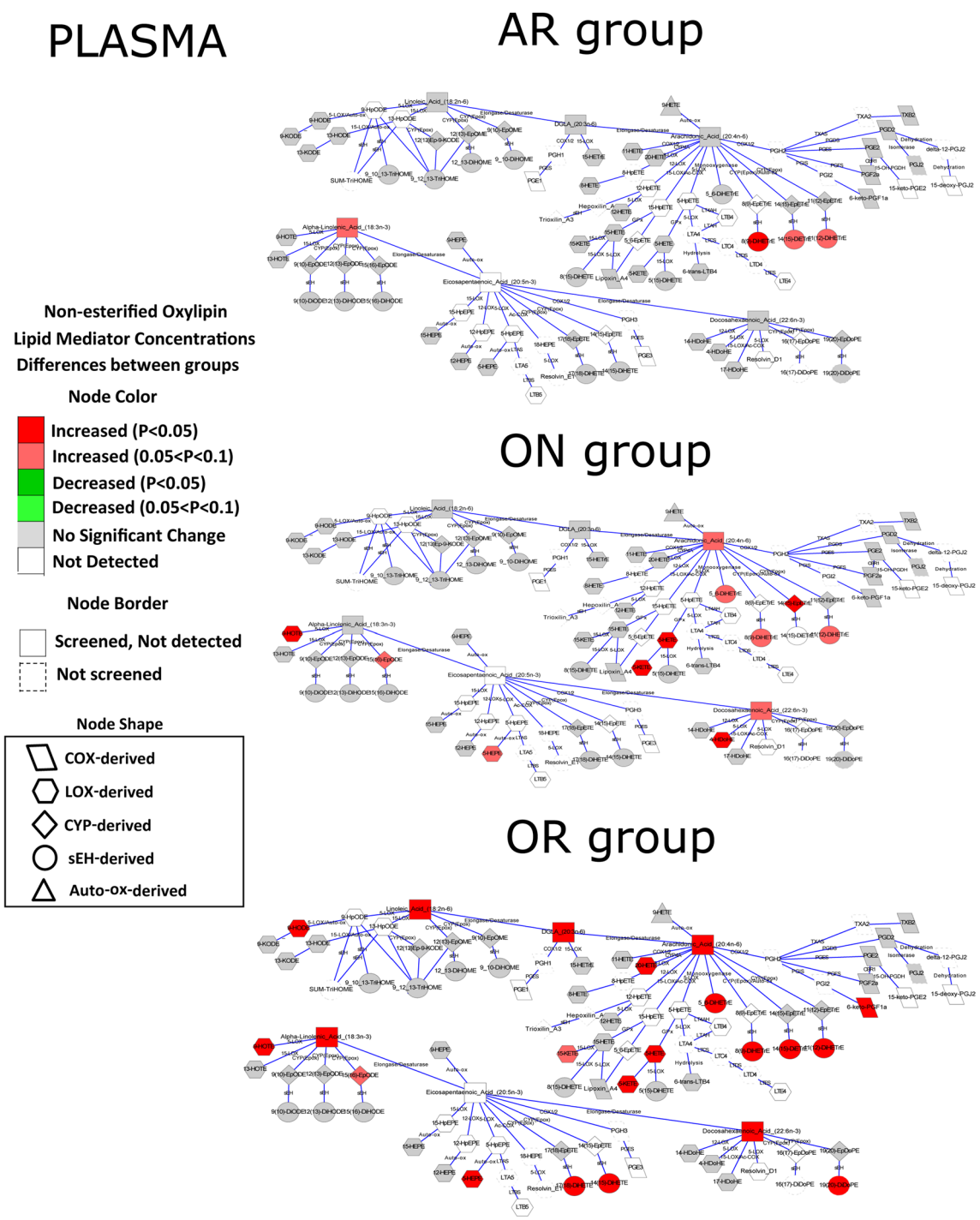

Fig. 5 Biochemical network displaying differences in circulating free oxylipins between AR, ON and OR relative to AN. Edge label represents the enzymes which mediates the respective biochemical transformation. Node color represents significance (*white*- not detected; *grey*-not statistically different; *green*- significantly decreased in group relative to AN; *red*- significantly increased in group relative to AN). Lighter shades of *red* and *green* were compounds changing with p-values > 0.05 but <0.1. Node shapes depicts the respective oxylipin metabolizing pathway. AN- normal food intake, normal air; AR- restricted food intake, normal air; ON- 75% oxygen, normal food intake; OR- 75% oxygen, restricted food intake

primary metabolites, biogenic amines and complex lipids, along with targeted analysis of lipid signaling mediators was utilized to characterize the metabolic perturbations that occur in SD rat pups exposed to two triggers for PH. Numerous metabolite changes in metabolic pathways and structural and signaling lipid compounds occurred,

implicating hyperoxia as the main cause of metabolic perturbations in the lung, while growth restriction, hyperoxia alone or the combination affected plasma metabolites.

The metabolic changes in the lung were largely confined to two groups undergoing hyperoxia, suggesting that disruption of lung metabolism was more driven by increased oxygen exposure than growth restriction. Many of these changes were associated with increased presence of ROS and reactive nitrogen species (RNS) characteristic of hyperoxia and further supported by our observation of increased 3-nitrotyrosine levels, an indirect measure of peroxynitrite. This is particularly relevant since ROS are known to have profound effects on vasculature remodeling and are strongly linked to the development of BPD and induction of PH (Farrow et al. 2010). The widespread metabolic effects included metabolic energy pathways contributing to ROS production, pathways impacted by the presence of ROS, and lipid profiles altered by ROS.

In regards to specific metabolic energy pathways, 3-hydroxybutyric acid, acyl-carnitines and many of the TCA cycle intermediates were elevated while total triglycerides were decreased in lung tissue of ON and OR rats compared to control suggesting increased fatty acid ß-oxidation and mitochondrial respiration while glycolysis intermediates were decreased and glucose was unchanged (Fig. 1e). Elevated fatty acid ß-oxidation is known to increase generation of ROS, particularly superoxide radicals, due to a higher rate of mitochondrial uncoupling (Qatanani and Lazar 2007; Brand et al. 2004).

Pathways impacted by the presence of ROS were the polyol (aldose reductase), nitric oxide, xanthine oxidase, glutathione, and pentose phosphate pathways (Fig. 1e). Elevated in the hyperoxic groups, sorbitol is produced from the oxidation of glucose by aldose reductase, an NADPH-dependent oxidoreductase. Overproduction of mitochondrial superoxide radicals has been shown to stimulate aldose reductase activity in models of diabetes (Nishikawa et al. 2000). Moreover, increased polyol pathway activity is a major contributor of oxidative-nitrosative stress (Obrosova et al. 2005) and linked to eNOS uncoupling (El-Remessy et al. 2003), consistent with our previously published results indicating alterations in nitrate/nitrite levels and eNOS expression (Wedgwood et al. 2016). Hyperoxia-associated decreases in xanthine and the antioxidant uric acid, an oxidation product of xanthine through xanthine oxidase known to neutralize superoxide and peroxynitrite, were observed (Hare and Johnson 2003; Pacher et al. 2006). Interestingly, although previous research mostly shows an upregulation of xanthine oxidase produces superoxides in response to hyerpoxia, evidence also supports that xanthine oxidase expression can be downregulated in circumstances of excess ROS and RNS through feedback inhibition by peroxynitite, a compound we confirmed to be elevated by follow-up testing (Pacher et al. 2006). Additionally, glutathione, an important endogenous antioxidant, was significantly reduced with hyperoxia whereas gluthathione disulfide, a byproduct of increased glutathione utilization, was significantly elevated. Furthermore, the decreased concentrations of glucose-6-phosphate, the initial substrate for the pentose phosphate pathway, and fructose-6-phosphate may have influenced pentose phosphate pathway activity as a source of NADPH for ROS scavenging and fatty acid synthesis.

Lung lipid profiles of structural and signaling compounds altered in the hyperoxic groups were associated with ROS included decreased plasmalogen PCs and lysoPCs and epoxides (Supplemental Figure S1A). It is interesting to note that plasmalogens are both a component of surfactant and can serve as an anti-oxidant to protect against ROS since the loss of pulmonary surfactant is a well-known risk marker for and contributor to development of BPD and consequent PH (Akella and Deshpande 2013; Yamashita et al. 2013). The efficient quenching of oxidants by vinyl ether prevents oxidation of polyunsaturated fatty acids, and thus breakdown products don't propogate lipid oxidation. This corroborates our observation of unchanged oxylipin ROS markers F2 isoprostanes and 9-HETE, perhaps suggesting plasmalogens were contributing to the protection of cellular membranes (Engelmann 2004). Decreased plasmalogen-PCs may also be related to activation of calcium independent phospholipase cPLA2. Plasmalogen-PCs are known to be rich in arachidonic acid and docosahexanoic acid at the sn-2 position, compounds we observed to be elevated (Braverman and Moser 2012). The increase in total esterified and non-esterified CYP450-derived epoxides in the hyperoxic groups can also be associated with increased ROS production since overexpression of CYP450 also produces superoxide radicals (Khan et al. 2007; Fleming et al. 2001; Viswanathan et al. 2003). It is also possible their concentration changes were partially related to abnormal oxygen exposure-related peripheral endothelial modulation of vessel wall smooth muscle cell (SMC) proliferation (Jankov et al. 2006; Zhang et al. 2012) contributing to pulmonary vascular remodeling. Since CYP450 oxylipins are primarily stored at the sn-1 position in SMC phosphatidylcholines and are thus resistant to PLA_2 (Fang et al. 2003), it may have been that sn-1 position CYP450 oxylipins were being retained in PCs while LOX oxylipins located at the sn-2 position were being released initially. This agrees with previous research indicating a sequential release of specific oxylipins during disease progression (Kiss et al. 2000) and our observed decrease in 12/15-LOX oxylipins in the presence of increased epoxides.

The circulating plasma metabolome was uniquely affected by growth restriction or hyperoxia and exhibited additive effects with combined treatment. In addition,

changes were not always in concert with the lung. Specifically, unlike the lung, circulating choline-containing total PCs and select sphingomyelins were significantly reduced in both growth restriction groups but were unchanged in the hyperoxic groups. (Supplemental Figure S1A; Supplemental Table S2). It is reasonable to hypothesize that the nutritional deprivation used to induce PNGR reduces availability of the nutrients required for phospholipid synthesis including choline, a hypothesis that can be easily tested in this model.

Observations unique to plasma metabolites in hyperoxic groups without PNGR-related additive effects included increases in oxylipins, including non-esterified oxylipins, several circulating sEH-derived diols, and 5-LOX-derived oxylipins (Supplemental Figure S1B). Increased concentrations of 5-LOX and sEH metabolites are associated with the development and presence of PH. In fact, release of diols into circulation is associated with increased systemic inflammation and blood pressure (Revermann 2010), impacting the function and health of a variety of organs.

Another interesting observation was the increase in circulating TMAO in the combined growth restriction and hyperoxia OR group, suggesting that the gut microbiome may also be altered in this model potentially increasing atherosclerosis risk (Bennett et al. 2013).

In agreement with the lung results, yet exhibiting an additive effect, were hyperoxia-induced increases in metabolic energy metabolites 3-hydroxybutyric acid and decreases in glucogenic amino acids and arginine (Figs. 1e, 3). This is a relevant observation since arginine deficiency and a reduction in nitric oxide (NO) production can act as facilitators of vasculature remodeling leading to the development of BPD and consequent PH (Gadhia et al. 2014; Pearson et al. 2001; Vadivel et al. 2010). Changes including increased acylcarnitines and decreased xanthine oxidase metabolites in hyperoxic groups were also similar to that seen in the lung, but did not exhibit an additive effect. Most highly correlative were levels of 3-hydroxybutyric acid, which had a strong positive association ($r = 0.953$; p-value < 0.001) between plasma and lung and could serve as stable biomarker of oxidative stress and PH severity (Supplemental Figure S3). Since the concentrations of this metabolite are impacted by a variety of organs, its fluctuations are likely more indicative of widespread metabolic perturbations throughout the body and cannot be attributed to the lungs alone.

Many of the metabolomics alterations observed are in accordance with our previous study with this model (Wedgwood et al. 2016). For example, we hypothesized previously that downregulated mTOR led to decreased HIF1α and VEGF expression and consequently decreased angiogenesis. This was partially supported by both a decrease in 4E-BP1 protein phosphorylation and a decrease in branched chain amino acids, known to positively regulate mTOR activity. Furthermore, 12-LOX oxylipins may upregulate HIF1α and contribute to increased angiogenesis (Krishnamoorthy and Honn 2011). Thus, decreased LOX product concentrations could have limited the contribution of HIF1a to angiogenesis, as evidenced by increased MWT, decreased lung vessel density, and increased SMC proliferation. The previously reported observations of increased ROS, decreased nitrate + nitrite, and decreased eNOS, are supported by numerous metabolite changes and increased peroxynitrite in our metabolomics analysis.

In order to follow up on the metabolomics results, further investigation into these different modes of PH induction should include: (1) their role in terms of altered energy metabolism in the form of increased beta-oxidation and mitochondrial respiration and decreased glycolysis, (2) the impact of implicated mechanisms such as aldose-reductase, xanthine oxidase, NADPH oxidase, glucose-6-phosphate dehydrogenase and CYP2, and (3) factors protecting against lipid peroxidation such as plasmalogen phospholipids in hyperoxia-induced PH. Differential treatment-induced metabolic changes between the lung and plasma raise questions regarding their impact on metabolically active tissues such as the liver.

In conclusion, the metabolomics results described in the current study, together with the phenotypic and gene expression results previously published provide further insight into the factors contributing to the development of BPD and PH. In spite of the small sample sizes, the relative differences between groups were large compared to the intra-group variance, which suggest that the observed effects can be extrapolated to a larger population. The rat model of hyperoxia in combination with PNGR may be a valuable tool for the continued investigation of this complex disease. Future metabolomics studies may identify temporal and gender-specific changes that will improve our understanding of the underlying mechanisms. Furthermore, analysis of umbilical cord blood samples from preterm infants with PH and BPD may identify biomarkers detectable at birth that predict the development of PH later in life.

Funding This research is funded by the National Institutes of Health grant U24 DK097154 (OF) through a pilot grant to SW, instrument Grant S10 RR031630 (OF) and by the USDA (Intramural Project 2032-51530-022-00D). The USDA is an equal opportunity employer and provider.

Compliance with ethical standards

Conflict of interest The authors declare no conflicts of interest in relation to the work described.

Ethical approval All procedures performed in studies involving animals were in accordance with the ethical standards of Institutional Animal Care and Use Committee at UC Davis.

Informed consent Informed consent was obtained from all individual participants included in the study.

References

Akella, A., & Deshpande, S. B. (2013). Pulmonary surfactants and their role in pathophysiology of lung disorders. *Indian Journal of Experimental Biology, 51*(1), 5–22.

Barupal, D. K., Haldiya, P. K., Wohlgemuth, G., Kind, T., Kothari, S. L., Pinkerton, K. E., et al. (2012). MetaMapp: mapping and visualizing metabolomic data by integrating information from biochemical pathways and chemical and mass spectral similarity. *BMC Bioinformatics, 13*(1), 99.

Benjamini, Y., & Hochberg, Y. (1995). Controlling the false discovery rate: a practical and powerful approach to multiple testing. *Journal of the Royal Statistical Society. Series B (Methodological)*, 289–300.

Bennett, B. J., de Aguiar Vallim, T. Q., Wang, Z., Shih, D. M., Meng, Y., Gregory, J., et al. (2013). Trimethylamine-N-oxide, a metabolite associated with atherosclerosis, exhibits complex genetic and dietary regulation. *Cell Metabolism, 17*(1), 49–60. doi:10.1016/j.cmet.2012.12.011.

Berkelhamer, S. K., Mestan, K. K., & Steinhorn, R. H. (2013). Pulmonary hypertension in bronchopulmonary dysplasia. *Seminars in Perinatology, 37*(2), 124–131. doi:10.1053/j.semperi.2013.01.009.

Bolton, E. E., Wang, Y., Thiessen, P. A., & Bryant, S. H. (2008). PubChem: integrated platform of small molecules and biological activities. *Annual Reports in Computational Chemistry, 4*, 217–241.

Brand, M. D., Affourtit, C., Esteves, T. C., Green, K., Lambert, A. J., Miwa, S., et al. (2004). Mitochondrial superoxide: production, biological effects, and activation of uncoupling proteins. *Free Radical Biology and Medicine, 37*(6), 755–767. doi:10.1016/j.freeradbiomed.2004.05.034.

Braverman, N. E., & Moser, A. B. (2012). Functions of plasmalogen lipids in health and disease. *Biochimica et Biophysica Acta, 1822*(9), 1442–1452. doi:10.1016/j.bbadis.2012.05.008.

Cao, Y., Charisi, A., Cheng, L.-C., Jiang, T., & Girke, T. (2008). ChemmineR: a compound mining framework for R. *Bioinformatics (Oxford, England), 24*(15), 1733–1734.

Check, J., Gotteiner, N., Liu, X., Su, E., Porta, N., Steinhorn, R., et al. (2013). Fetal growth restriction and pulmonary hypertension in premature infants with bronchopulmonary dysplasia. *Journal of Perinatology: Official Journal of the California Perinatal Association, 33*(7), 553–557. doi:10.1038/jp.2012.164.

DeviumWeb: Dynamic Multivariate Data Analysis and Visualization Platform [computer program]. 2014 doi:10.1042/bj20141455.

El-Remessy, A. B., Abou-Mohamed, G., Caldwell, R. W., & Caldwell, R. B. (2003). High glucose-induced tyrosine nitration in endothelial cells: role of eNOS uncoupling and aldose reductase activation. *Investigative Ophthalmology and Visual Science, 44*(7), 3135–3143.

Engelmann, B. (2004). Plasmalogens: targets for oxidants and major lipophilic antioxidants. *Biochemical Society Transactions, 32*(1), 147–150. doi:10.1042/bst0320147.

Fahrmann, J., Grapov, D., Yang, J., Hammock, B., Fiehn, O., Bell, G. I., et al. (2015). Systemic Alterations in the Metabolome of Diabetic NOD Mice Delineate Increased Oxidative Stress Accompanied by Reduced Inflammation and Hypertriglyceridemia. *American Journal of Physiology-Endocrinology and Metabolism*, ajpendo.00019.02015, doi:10.1152/ajpendo.00019.2015.

Fang, X., Weintraub, N. L., & Spector, A. A. (2003). Differences in positional esterification of 14,15-epoxyeicosatrienoic acid in phosphatidylcholine of porcine coronary artery endothelial and smooth muscle cells. *Prostaglandins & Other Lipid Mediators, 71*(1–2), 33–42.

Farrow, K. N., Wedgwood, S., Lee, K. J., Czech, L., Gugino, S. F., Lakshminrusimha, S., et al. (2010). Mitochondrial oxidant stress increases PDE5 activity in persistent pulmonary hypertension of the newborn. *Respiratory Physiology & Neurobiology, 174*(3), 272–281. doi:10.1016/j.resp.2010.08.018.

Fiehn, O., Wohlgemuth, G., & Scholz, M. (2005). Setup and annotation of metabolomic experiments by integrating biological and mass spectrometric metadata. *Data Integration in the Life Sciences, Proceedings, 3615*, 224–239.

Fiehn, O., Wohlgemuth, G., Scholz, M., Kind, T., Lee do, Y., Lu, Y., et al. (2008). Quality control for plant metabolomics: reporting MSI-compliant studies. [Research Support, N.I.H., Extramural Research Support, U.S. Gov't, Non-P.H.S.]. *Plant Journal, 53*(4), 691–704, doi:10.1111/j.1365-313X.2007.03387.x.

Fleming, I., Michaelis, U. R., Bredenkotter, D., Fisslthaler, B., Dehghani, F., Brandes, R. P., et al. (2001). Endothelium-derived hyperpolarizing factor synthase (Cytochrome P450 2C9) is a functionally significant source of reactive oxygen species in coronary arteries. *Circulation Research, 88*(1), 44–51.

Gadhia, M. M., Cutter, G. R., Abman, S. H., & Kinsella, J. P. (2014). Effects of early inhaled nitric oxide therapy and vitamin A supplementation on the risk for bronchopulmonary dysplasia in premature newborns with respiratory failure. *The Journal of Pediatrics, 164*(4), 744–748. doi:10.1016/j.jpeds.2013.11.040.

Grapov, D. (2014). MetaMapR: Metabolomic Mapping and Analysis Tools. *version 1.3.1*, https://github.com/dgrapov/MetaMapR, doi:10.5281/zenodo.12880.

Grapov, D., Adams, S. H., Pedersen, T. L., Garvey, W. T., & Newman, J. W. (2012). Type 2 diabetes associated changes in the plasma non-esterified fatty acids, oxylipins and endocannabinoids. *PLoS ONE, 7*(11), e48852. doi:10.1371/journal.pone.0048852.

Hare, J. M., & Johnson, R. J. (2003). Uric acid predicts clinical outcomes in heart failure: insights regarding the role of xanthine oxidase and uric acid in disease pathophysiology. *Circulation, 107*(15), 1951–1953. doi:10.1161/01.cir.0000066420.36123.35.

Jankov, R. P., Kantores, C., Belcastro, R., Yi, M., & Tanswell, A. K. (2006). Endothelin-1 inhibits apoptosis of pulmonary arterial smooth muscle in the neonatal rat. *Pediatric Research, 60*(3), 245–251. doi:10.1203/01.pdr.0000233056.37254.0b.

Jou, M. Y., Lonnerdal, B., & Griffin, I. J. (2013). Effects of early postnatal growth restriction and subsequent catch-up growth on body composition, insulin sensitivity, and behavior in neonatal rats. *Pediatric Research, 73*(5), 596–601. doi:10.1038/pr.2013.27.

Khan, M., Mohan, I. K., Kutala, V. K., Kumbala, D., & Kuppusamy, P. (2007). Cardioprotection by sulfaphenazole, a cytochrome p450 inhibitor: mitigation of ischemia-reperfusion injury by scavenging of reactive oxygen species. *The Journal of Pharmacology and Experimental Therapeutics, 323*(3), 813–821. doi:10.1124/jpet.107.129486.

Kind, T., Tolstikov, V., Fiehn, O., & Weiss, R. H. (2007). A comprehensive urinary metabolomic approach for identifying kidney cancerr. *Analytical Biochemistry, 363*(2), 185–195. doi:10.1016/j.ab.2007.01.028.

Kiss, L., Schutte, H., Mayer, K., Grimm, H., Padberg, W., Seeger, W., et al. (2000). Synthesis of arachidonic acid-derived lipoxygenase and cytochrome P450 products in the intact human lung vasculature. *American Journal of Respiratory and Critical Care Medicine, 161*(6), 1917–1923. doi:10.1164/ajrccm.161.6.9906058.

Kotera, M., Hirakawa, M., Tokimatsu, T., Goto, S., & Kanehisa, M. (2012). The KEGG databases and tools facilitating omics analysis: latest developments involving human diseases and

pharmaceuticals. In *Next Generation Microarray Bioinformatics* (pp. 19–39):New York: Springer.

Krishnamoorthy, S., & Honn, K. V. (2011). Eicosanoids and other lipid mediators and the tumor hypoxic microenvironment. *Cancer and Metastasis Reviews, 30*(3–4), 613–618. doi:10.1007/s10555-011-9309-9.

Luria, A., Weldon, S. M., Kabcenell, A. K., Ingraham, R. H., Matera, D., Jiang, H., et al. (2007). Compensatory mechanism for homeostatic blood pressure regulation in Ephx2 gene-disrupted mice. *The Journal of Biological Chemistry, 282*(5), 2891–2898. doi:10.1074/jbc.M608057200.

Mirza, H., Ziegler, J., Ford, S., Padbury, J., Tucker, R., & Laptook, A. (2014). Pulmonary hypertension in preterm infants: prevalence and association with bronchopulmonary dysplasia. *The Journal of Pediatrics, 165*(5), 909–914.e901. doi:10.1016/j.jpeds.2014.07.040.

Mourani, P. M., Sontag, M. K., Younoszai, A., Miller, J. I., Kinsella, J. P., Baker, C. D., et al. (2015). Early pulmonary vascular disease in preterm infants at risk for bronchopulmonary dysplasia. *American Journal of Respiratory and Critical Care Medicine, 191*(1), 87–95. doi:10.1164/rccm.201409-1594OC.

Nishikawa, T., Edelstein, D., Du, X. L., Yamagishi, S., Matsumura, T., Kaneda, Y., et al. (2000). Normalizing mitochondrial superoxide production blocks three pathways of hyperglycaemic damage. *Nature, 404*(6779), 787–790. doi:10.1038/35008121.

Obrosova, I. G., Pacher, P., Szabo, C., Zsengeller, Z., Hirooka, H., Stevens, M. J., et al. (2005). Aldose reductase inhibition counteracts oxidative-nitrosative stress and poly(ADP-ribose) polymerase activation in tissue sites for diabetes complications. *Diabetes, 54*(1), 234–242.

Pacher, P., Nivorozhkin, A., & Szabo, C. (2006). Therapeutic effects of xanthine oxidase inhibitors: renaissance half a century after the discovery of allopurinol. *Pharmacological Reviews, 58*(1), 87–114. doi:10.1124/pr.58.1.6.

Pearson, D. L., Dawling, S., Walsh, W. F., Haines, J. L., Christman, B. W., Bazyk, A., et al. (2001). Neonatal pulmonary hypertension–urea-cycle intermediates, nitric oxide production, and carbamoyl-phosphate synthetase function. *The New England Journal of Medicine, 344*(24), 1832–1838. doi:10.1056/nejm200106143442404.

Picklo, M. J. Sr., & Newman, J. W. (2015). Antioxidant supplementation and obesity have independent effects on hepatic oxylipin profiles in insulin-resistant, obesity-prone rats. *Free Radical Biology and Medicine, 89*, 182–191. doi:10.1016/j.freeradbiomed.2015.07.152.

Qatanani, M., & Lazar, M. A. (2007). Mechanisms of obesity-associated insulin resistance: many choices on the menu. *Genes and Development, 21*(12), 1443–1455. doi:10.1101/gad.1550907.

Revermann, M. (2010). Pharmacological inhibition of the soluble epoxide hydrolase-from mouse to man. *Current Opinion in Pharmacology, 10*(2), 173–178. doi:10.1016/j.coph.2009.12.002.

Robbins, I. M., Moore, T. M., Blaisdell, C. J., & Abman, S. H. (2012). National Heart, Lung, and Blood Institute Workshop: improving outcomes for pulmonary vascular disease. *Circulation, 125*(17), 2165–2170. doi:10.1161/circulationaha.112.092924.

Rozance, P. J., Seedorf, G. J., Brown, A., Roe, G., O'Meara, M. C., Gien, J., et al. (2011). Intrauterine growth restriction decreases pulmonary alveolar and vessel growth and causes pulmonary artery endothelial cell dysfunction in vitro in fetal sheep. *American Journal of Physiology. Lung Cellular and Molecular Physiology, 301*(6), L860–L871. doi:10.1152/ajplung.00197.2011.

Scholz, M., & Fiehn, O. (2007). SetupX–a public study design database for metabolomic projects. *Pacific Symposium Biocomputing*, 169–180.

Shannon, P., Markiel, A., Ozier, O., Baliga, N. S., Wang, J. T., Ramage, D., et al. (2003). Cytoscape: A software environment for integrated models of biomolecular interaction networks. *Genome Research, 13*(11), 2498–2504.

Slaughter, J. L., Pakrashi, T., Jones, D. E., South, A. P., & Shah, T. A. (2011). Echocardiographic detection of pulmonary hypertension in extremely low birth weight infants with bronchopulmonary dysplasia requiring prolonged positive pressure ventilation. *Journal of Perinatology: Official Journal of the California Perinatal Association, 31*(10), 635–640. doi:10.1038/jp.2010.213.

Strassburg, K., Huijbrechts, A. M., Kortekaas, K. A., Lindeman, J. H., Pedersen, T. L., Dane, A., et al. (2012). Quantitative profiling of oxylipins through comprehensive LC-MS/MS analysis: application in cardiac surgery. *Analytical and Bioanalytical Chemistry, 404*(5), 1413–1426. doi:10.1007/s00216-012-6226-x.

Sud, M., Fahy, E., Cotter, D., Azam, K., Vadivelu, I., Burant, C., et al. (2015). Metabolomics Workbench: An international repository for metabolomics data and metadata, metabolite standards, protocols, tutorials and training, and analysis tools. *Nucleic Acids Research*. doi:10.1093/nar/gkv1042.

Svensson, O., Kourti, T., & MacGregor, J. F. (2002). An investigation of orthogonal signal correction algorithms and their characteristics. *Journal of Chemometrics, 16*, 176–188.

Vadivel, A., Aschner, J. L., Rey-Parra, G. J., Magarik, J., Zeng, H., Summar, M., et al. (2010). L-citrulline attenuates arrested alveolar growth and pulmonary hypertension in oxygen-induced lung injury in newborn rats. *Pediatric Research, 68*(6), 519–525. doi:10.1203/PDR.0b013e3181f90278.

Viswanathan, S., Hammock, B. D., Newman, J. W., Meerarani, P., Toborek, M., & Hennig, B. (2003). Involvement of CYP 2C9 in mediating the proinflammatory effects of linoleic acid in vascular endothelial cells. *Journal of the American College of Nutrition, 22*(6), 502–510.

Wedgwood, S., Warford, C., Agvateesiri, S. C., Thai, P., Berkelhamer, S. K., Perez, M., et al. (2016). Postnatal Growth Restriction Augments Oxygen-Induced Pulmonary Hypertension in a Neonatal Rat Model of Bronchopulmonary Dysplasia. *Pediatric Research, 80*(6), 894–902.

Xia, J. & Wishart, D.S. (2016) Using MetaboAnalyst 3.0 for Comprehensive Metabolomics Data Analysis. *Current Protocols in Bioinformatics*, 55:14.10.1–14.10.91.

Yamashita, C. M., Veldhuizen, R. A. W., & Gill, S. E. (2013). Alveolar macrophages and pulmonary surfactant—more than just friendly neighbours. *OA Biology, 1*(1), 6.

Zhang, J., Hu, H., Palma, N. L., Harrison, J. K., Mubarak, K. K., Carrie, R. D., et al. (2012). Hypoxia-induced endothelial CX3CL1 triggers lung smooth muscle cell phenotypic switching and proliferative expansion. *American Journal of Physiology. Lung Cellular and Molecular Physiology, 303*(10), L912–L922. doi:10.1152/ajplung.00014.2012.